ORIGINAL ARTICLE

Age-related compositional changes and correlations of gut microbiome, serum metabolome, and immune factor in rats

Xia Zhang · Yuping Yang · Juan Su · Xiaojiao Zheng · Chongchong Wang · Shaoqiu Chen · Jiajian Liu · Yingfang Lv · Shihao Fan · Aihua Zhao · Tianlu Chen · Wei Jia · Xiaoyan Wang

Abstract Aging is a complex physiological process associated with degenerative disorder of metabolism and immune function, which contributes to the occurrence of senile diseases. The gut microbiota affects systemic inflammation in aging processes probably through metabolism, but their relationship is still unclear. In this study, 16S-rRNA-sequencing technology, gas chromatography-time-of-flight mass spectrometry (GC-TOFMS)–based metabolic profiling, and immune factor analysis combined with advanced differential and association analysis were employed to investigate the correlation between the microbiome, metabolome, and immune factors in male Wistar rats across lifespan. Our findings showed significant changes in the ileum microbiome and serum metabolome compositions across aging process. A two-level strategy was applied to demonstrate that key metabolites associated with age such as 4-hydroxyproline, proline, and lysine were clustered together and positively correlated with beneficial microbes including *Bifidobacterium*, *Lactobacillus*, and *Akkermansia*. Function analysis explored association between serum metabolite class and specific gut bacteria's metabolism pathways. Further correlation analysis on all the alteration patterns provided an interaction network of main immune factors such as IL-10, IgA, IgM, and IgG with key gut bacteria and serum metabolites. This study offers new insights into the relationship between immune factors, serum metabolome, and the gut microbiome.

Xia Zhang, Yuping Yang, and Juan Su equally contributed to this study as first authors.

Electronic supplementary material The online version of this article (https://doi.org/10.1007/s11357-020-00188-y) contains supplementary material, which is available to authorized users.

X. Zhang · Y. Yang · C. Wang · S. Chen · Y. Lv ·
X. Wang (✉)
Key Laboratory of Systems Biomedicine(Ministry of Education), Shanghai Center for Systems Biomedicine, Shanghai Jiao Tong University, Shanghai 200240, China
e-mail: cathywxy@sjtu.edu.cn

J. Su · S. Fan
College of Veterinary Medicine, Nanjing Agriculture University, Nanjing 210095, China

X. Zheng · J. Liu · A. Zhao · T. Chen (✉) · W. Jia (✉)
Shanghai Key Laboratory of Diabetes Mellitus and Center for Translational Medicine, Shanghai Jiao Tong University Affiliated Sixth People's Hospital, Shanghai 200233, China
e-mail: chentianlu@sjtu.edu.cn
e-mail: weijia@sjtu.edu.cn

Introduction

Aging is a physiological process involving complex interdependent network systems and contributes to the onset and progression of senile diseases such as cardiovascular disease, Alzheimer's disease (AD), arthritis, and diabetes (Butler et al. 2008; Wijsman et al. 2011). Age-related decrease in gut microbiota diversity has been reported among the elderly, and this has been linked to an increase in the risk of different diseases.

Bifidobacterium spp. and *Lactobacillus* spp. are more abundant during the early stages of life and decrease in old age (Hor et al. 2019; Singh et al. 2019). Gut flora plays a critical role of imbalance in senescence and premature death of progeria animals, and the dysbacteriosis could be significantly improved by transplantation of normal fecal bacteria or supplementation with Akk bacteria. Although the mechanisms for these changes have not been clarified, metabolic regulation may act a pivotal part in senescence regulation by intestinal flora (Bárcena et al. 2019).

From the first day of life, the gut microbiota functions in metabolism and supports growth, development, maturity, and aging (Chen et al. 2019; Korpela et al. 2019; Ticinesi et al. 2019). Gut microbial metabolites are important signaling molecules associated with the occurrence of a number of diseases such as cancer and cardiovascular diseases (Kurilshikov et al. 2019). In 2016, we explored brain metabolome, revealing gut flora–related metabolites which were detected dramatically changing in rat brain with age (Zheng et al. 2016). Subsequently, we proposed a strategy association study of brain metabolome and gut microbiome across the lifespan of rats (Chen et al. 2018). These two studies provide appropriate approaches to data analysis and association of metabolome and microbiome, expanding our understanding of the microbial-metabolite relationship.

Aging is characterized by chronic, low-grade systemic inflammation referred to as inflammaging which contributes to the pathogenesis of age-related diseases (Ferrucci and Fabbri 2018; Sansoni et al. 2008). Changes in immune cytokines have been closely related to the occurrence and development of senile diseases (Castaneda-Delgado et al. 2017), whereas the causes of this low-grade inflammation and its specific regulatory mechanism are still unclear. Recent studies suggest that the gut bacteria may play a crucial role in these age-related inflammations (Buford 2017). However, the linkage between the immune system, gut microbiota, and metabolites throughout the aging process has not been established. Identifying the relationship between the immune system and the gut microbiota can help to promote healthy aging and also provide new approaches to anti-aging.

The current study explored the relationship between immune factors, serum metabolome, and gut microbiota in male Wistar rats at different time points (weeks 1, 3, 7, 9, 12, 56, 111). The study utilized a three-pronged association study coupled with immunologic factor analysis, serum metabolic profiling, and microbiome analysis. The dual-omics data were extracted and clustered into groups with different changing characteristics (Pedersen et al. 2018). Spearman's correlation analysis and network were used to determine the immune factor-metabolite-bacterium correlation pairs. This provides an understanding of the relationship between immune factors, serum metabolome, and gut microbiome at different aging processes.

Materials and methods

Animal handling and sample collection

All experiments were carried out strictly in accordance with recommendations on the National Institutes of Health's Guide for Care and Use of Laboratory Animals. The experimental program was approved by the Center for Laboratory Animals of Shanghai Jiao Tong University.

The whole experimental workflow is summarized in Fig. 1. Briefly, male Wistar rats were all born by the seven mother rats purchased from Shanghai Laboratory Animal Co, Ltd. (SLAC, Shanghai, China). Six newborn rats were randomly selected from each litter and randomly assigned to each group. All laboratory rats were fed in a clean environment under the condition of 12-h light/12-h dark cycle at 20–22 °C and $45 \pm 5\%$ humidity. Also, all rats were given free sterile chow and water. The diet composition of standard chow is provided in Table S1. A total of 42 male Wistar rats were allotted to 7 groups (weeks 1, 3, 7, 9, 12, 56, and 111 after birth, represented by W1, W3, W7, W9, W12, W56, and W111, $n = 6$ per group). Blood, whole spleen, and intestinal content samples were collected from each rat at the end of the corresponding time point. Blood sample was extracted from the tail vein and then centrifuged at 4 °C, 3000 rpm for 20 min; the supernatant was transferred to a fresh tube. All samples were immediately stored at − 80 °C pending analysis.

GC/TOF-MS sample preparation and assessment

Serum metabolomics pretreatment and measurement were performed according to the procedures established in our laboratory (Hou et al. 2015; Zhang et al. 2016). Briefly, 300 μL of a precooled mixed solvent

(V_{methanol}:$V_{\text{chloroform}}$ = 3:1) was added to 50 μL serum in a 1.5-mL centrifuge tube, followed by vortex oscillation for 30 s. Then, the mixture was arranged in −20 °C for 10 min and centrifuged at 1000 rpm for 10 min. A total of 300 μL supernatant was transferred into a new vial with L-2-chlorophenylalanine (0.1 mg/mL, 10 μL) as the internal standard. Afterward, the supernatant was dried under vacuum at room temperature and dissolved by 80 μL methoxamine (15 mg/mL in pyridine). After vortex oscillation for 30 s, the sample vial was stored at 30 °C for 90 min. Finally, the sample vial was added with 50 μL of bis(trimethylsilyl)trifluoroacetamide (containing 1% trimethylchlorosilane) and kept at 70 °C for 60 min. The sample vials were kept at room temperature for 1 h before mass spectrometry analysis.

All samples were randomly injected to minimize systematic deviations. Quality control (QC) samples were prepared by pooling all plasma samples and used for all analytical methods. A mixed extraction of QC sample was subjected to assessment every ten sample injections.

Metabolite profiling was acquired using gas chromatography-time-of-flight mass spectrometry (GC/TOF-MS, LECO, USA) platform and preprocessed by Chroma TOF (LECO, USA). Compounds were identified using in-house and online libraries, such as the Human Metabolome Database (HMDB) and the National Institute of Standards and Technology (NIST). The final dataset included compound name, peak area, and retention time. Annotated metabolites with zero values in more than 60% samples were excluded. The mean value of corresponding variables was used to complete the missing value. A total of 82 metabolites were obtained, which were normalized into the total peak abundance of all metabolites in each sample before statistical analysis. They were then divided into 5 metabolite types according to their chemical structure.

Ileum content microbiota assessment

The ileum contents were removed from storage. Microbial DNA was extracted using the QIAamp Stool Mini kit (Qiagen, cat. no. 51504). The V4 hypervariable region of 16SrRNA was chosen as the PCR amplified region. The bacterial forward primer was 5′-AYTGGGYDTAAAGNG-3′ and the reverse primer was 5′-TACNVGGGTATCTAATCC-3′. The PCR conditions were set as follows: one predenaturation cycle at 94 °C for 4 min, 25 cycles of denaturation at 94 °C for 30 s, annealing at 50 °C for 45 s, elongation at 72 °C for 30 s, and one post-elongation cycle at 72 °C for 5 min. The amplified PCR products were separated on 0.8% agarose gels and extracted. The PCR products without primer dimers and contaminant bands were included for sequencing by Illumina Miseq platform.

The original data obtained by sequencing was saved in a paired-end FASTQ format and performed with QIIME 2 (version 2019.4) (Bolyen et al. 2018) with minor modification according to the official tutorials (https://docs.qiime2.org/2019.4/tutorials/). Raw reads were demultiplexed with no error in the index sequence. The DATA2 (Callahan et al. 2016) was used to obtain quality filtered, denoised, chimera-free, and merged amplicon sequence variants (ASVs). Sequences with any ambiguous based were excluded. Taxonomic annotation of ASVs was obtained in the Greengenes database (DeSantis et al. 2006). Alpha diversity metrics and beta diversity metrics were estimated using the diversity plugin. ASVs with richness in less than 0.001 % total reads or with zero values more than 80% of samples were removed. In this study, 427 ASVs under 16 phyla were reserved for subsequent analysis. PICRUst2 (Phylogenetic Investigation of Communities by Reconstruction of Unobserved States) together with KEGG (Kyoto Encyclopedia of Genes and Genomes) pathway library were applied to obtain predicted function matrix (Douglas et al. 2019). A total of 127 functions that related to metabolism were kept for analysis.

Measurement of immune factors and cytokines in the spleen

The levels of immune factors (IL-2, IL-4, IL-10), immunoglobulins (IgA, IgG, IgM), and NK cell in spleen samples were measured by the Rat interleukin-2 (IL-2) ELISA Kit, Rat interleukin-4 (IL-4) ELISA Kit, and Rat interleukin-10 (IL-10) ELISA Kit; Rat immunoglobulin A (IgA) ELISA Kit, immunoglobulin G (IgG) ELISA Kit, and immunoglobulin M (IgM) ELISA Kit; and NK cell ELISA Kit (Shanghai Jianglai Biotech, Shanghai, China). All steps followed the manufacturer's instructions.

Statistical analysis

The data matrix was imported into SIMCA-P 13.0 (Umetrics, Sweden) for principal component analysis (PCA) and partial least squares discriminant analysis
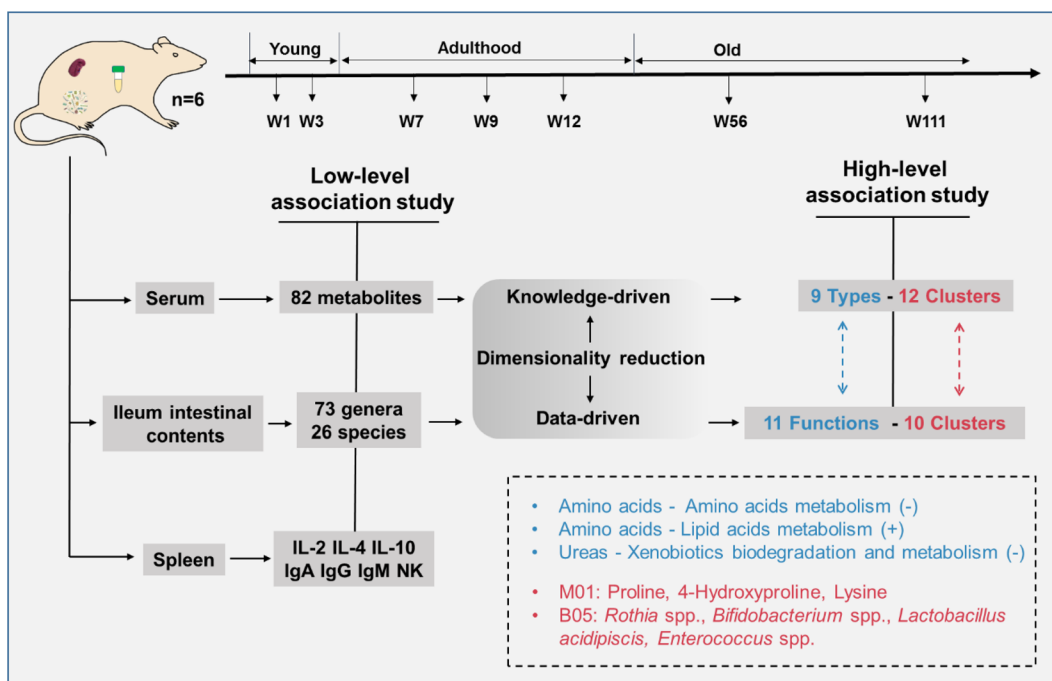
Fig. 1 Overview of the workflow integrating serum metabolome, gut microbiome, and spleen cytokines in rats among different age groups. After preprocessing raw metabolome and microbiome data, metabolites and microbiota are separately collapsed into co-abundance clusters. After which the clusters are filtered for statistically significant associations with age. Finally, the resulting clusters are taken for cross-domain association study

(PLS-DA) analyses, which were constructed using the GC-MS data as the X variable and the age as the Y variable. Also, principal coordinate analysis (PCoA) based on unweighted and weighted UniFrac OTU matrix was performed. MetaboAnalyst 3.0, GraphPad Prism 5.0 (6.0, GraphPad, USA), and R program (version 3.5, https://www.r-project.org/) were used for data analysis. Significant differences in variances among all seven groups were identified by the Kruskal-Wallis test as over 85% of the variables did not conform to normal distribution, followed by Dunn's post hoc test using a Benjamini-Hochberg false discovery rate (FDR) for multiple testing. Data in figures were presented as mean ± SEM. All tests were two-sided, the p values were corrected using FDR, and $p < 0.05$ was considered statistically significant.

Association analysis

We applied a two-level strategy to determine the associations between the serum metabolome and gut microbiome. For the high-level association study, two dimensionality reduction methods were used: (1) for knowledge-driven, correlations of metabolite types and predicted metabolic function–derived bacterial data were tested; (2) for data-driven, the integration and association study of intestinal microbiome data and serum metabolome data was performed according to the computational protocol with modifications (Pedersen et al. 2018). Firstly, we collapsed co-abundant serum metabolites into metabolite clusters (labeled M01-M12) using the R package WGCNA (weighted gene co-expression network analysis) (Langfelder and Horvath 2008) (Fig. 1). Signed, weighted co-abundance correlation (biweight midcorrelations after $\log_2$ transformation) networks were calculated across all metabolites. The resulting cluster eigenvector was presented to the profile of each metabolite cluster. The parameters were set in line with the details of the

Fig. 2 The effects of age on the serum metabolome. **a** The relative ▶ abundance of metabolite types in infancy, adulthood, and old age. The pie charts were normalized by samples groups. **b** The principal component analysis (PCA) performed based on each serum metabolite from all age groups. The boxplots of relative abundance of significantly changed metabolites of **c** amino acid metabolism, **d** carbohydrate metabolism, and **e** fatty acid metabolism in rats among the lifespan ($n = 6$). $^+p < 0.05$, $^*p < 0.01$, and $^{**}p < 0.001$ when compared with W7 by Dunn's test
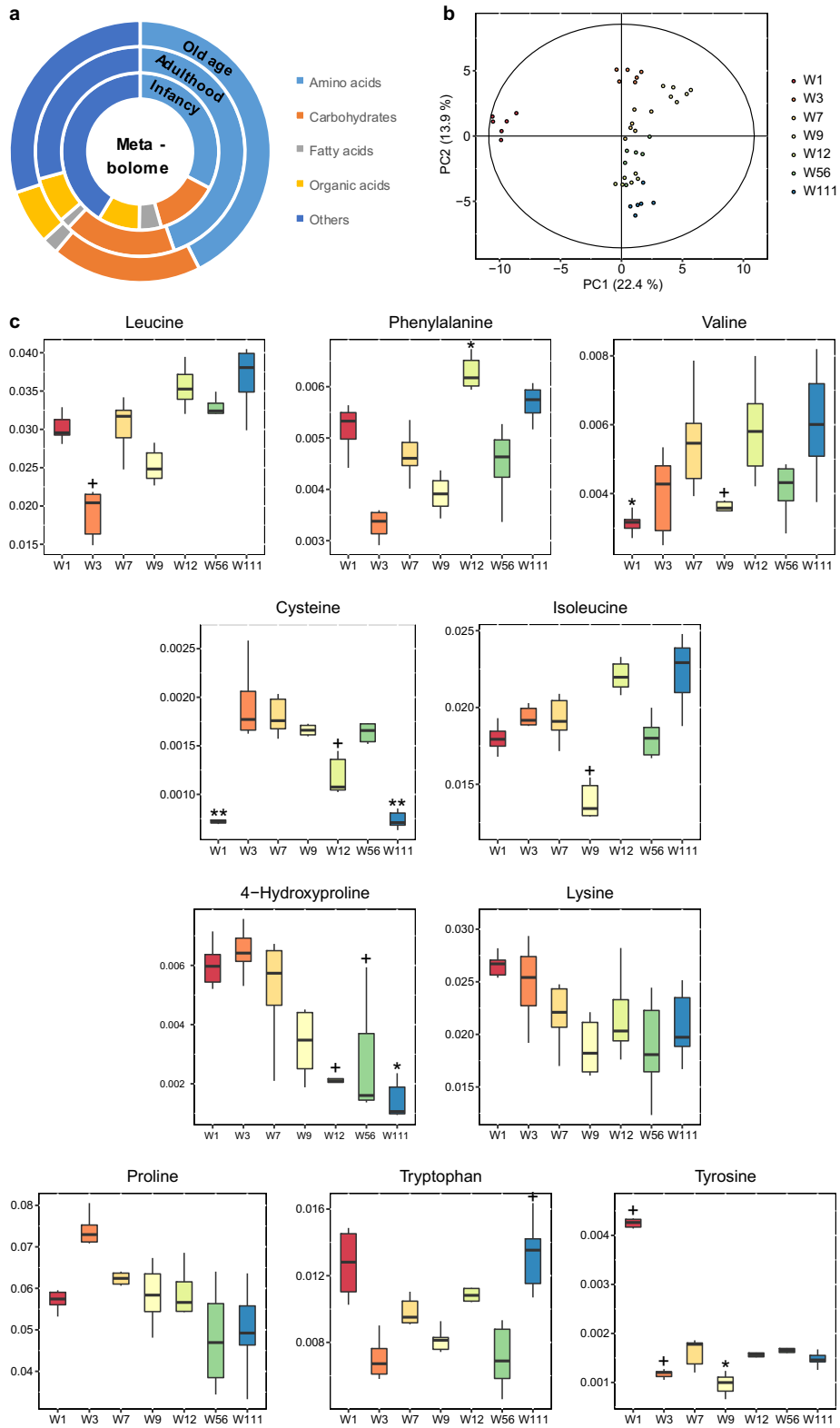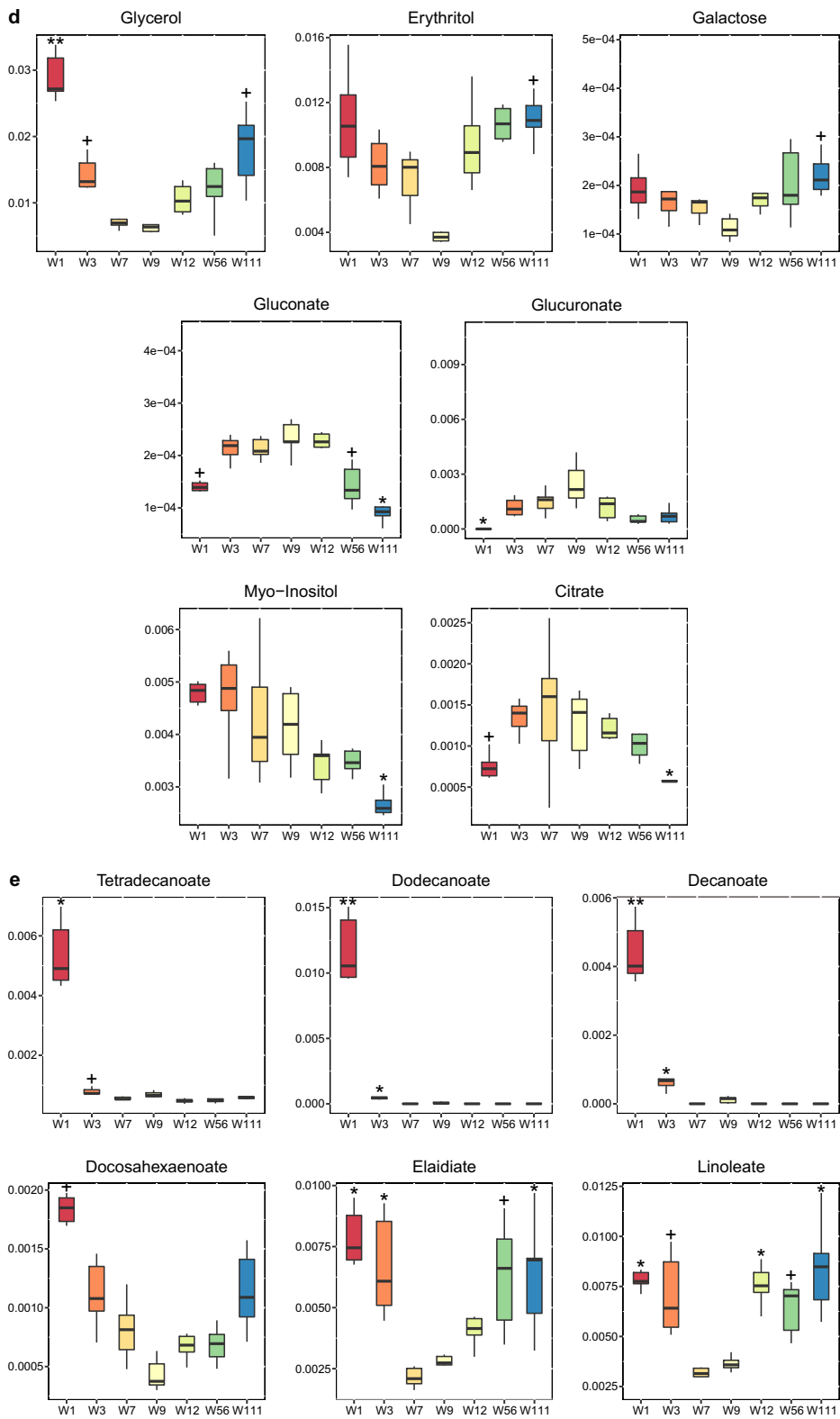
Fig. 2 (continued)

polar metabolites clustering in the published paper (Pedersen et al. 2018). Secondly, the microbiota data was summarized to microbiota clusters (labeled B01-B10) using the same method of metabolites. Thirdly, in the age-filtering step, age-related clusters were filtered by Spearman's correlation analysis with $p < 0.05$ and FDR < 0.1 and the resulting clusters were taken for cross-domain association analyses between metabolomics and microbiome. For the low-level association study, the associations among specified metabolite, bacterium, and cytokines were listed. Spearman's rank correlation coefficients were calculated using the cor.test function (method = "spearman") and were plotted with the pheatmap function in the package of R program. The significant correlation pairs were depicted in Cytoscape (3.4.0).

Results

Profiling of serum metabolites in rats by GC/TOF-MS

A total of 82 metabolites were identified by GC/TOF-MS, including 24 amino acids, 15 carbohydrates, 11 fatty acids, 19 organic acids, and 13 other small molecules. Amino acids and carbohydrates were the predominant types of metabolites, which account 62% of all metabolites (Fig. 2a). PCA was performed to characterize the global metabolomics differences among groups. The PCA score plot showed that the profile at 1 week was significantly different from other age groups (Fig. 2b). The profiles of all age groups can be clearly separated by the first and second principal components. Unsupervised analysis of serum groups showed that age was the predominant factor to the metabolic profile of healthy rats. This observation was also confirmed by the PLS-DA model at all age groups (Fig. S1a).

In order to find out the variables that contribute to the separation of serum metabolome, we further evaluated the alterations of aging on specific metabolites. Metabolites that showed significantly differences among 7 time points by the Kruskal-Wallis test were included. Several amino acids including leucine, phenylalanine, valine, and isoleucine increased while 4-hydroxyproline, lysine, and proline decreased with age (Fig. 2c). Interestingly, the levels of several carbohydrates showed a separation at the age of week 9. For example, glycerol, erythritol, and galactose decreased

from W1 to W9 and increased from W9 to W111. Gluconate and glucuronate increased from W1 to W9 and decreased from W9 to W111 (Fig. 2d). The levels of tetradecanoate, dodecanoate, decanoate, and docosahexaenoate were extremely high at W1 compared with other age groups. Docosahexaenoate, elaidiate, and linoleate decreased from W1 to W9 and increased from W9 to W111 (Fig. 2e).

Composition of intestinal microbiota in rats by 16S rRNA

Using the 16S rRNA sequencing, a total of 73 genera and 26 species were annotated among the 427 ASVs, which were present in at least 60% of the samples. Alpha diversity metrics and beta diversity metrics were estimated in Fig. S1c. In the phylum level, Firmicutes and Proteobacteria were the most predominant bacterial phyla found in ileum, followed by Bacteroidetes, Actinobacteria, Acidobacteria, and Verrucomicrobia (Fig. 3a). The relative abundance of Firmicutes was almost equal to Proteobacteria at the infancy, and then, Firmicutes increased and Proteobacteria decreased with age. The relative abundance of Firmicutes was positively correlated with age, while other phyla negatively correlated with age, such as Bacteroidetes, Proteobacteria, and Actinobacteria (Fig. 3a).

To characterize the global differences in gut microbiota composition among all seven groups, PCoA analysis was performed based on the unweighted and weighted UniFrac distances of the microbiota to visualize the clustering of all rats. From the PCoA plots shown in Fig. 3b, the composition of the ileum microbiota was dramatically changed from W1 to W111. The PCoA plot based on weighted UniFrac was depicted in Fig. S1b.

To explore the detailed gut microbiota composition, we analyzed the relative abundance of the dominant genera and species which were different in all groups (tested by the Kruskal-Wallis test with p value < 0.05). The levels of *Rhodococcus* spp., *Actinobacillus* spp., and *Bacillus* spp. were enriched in the aged rats. The relative abundance of *Bifidobacterium* spp., *Lactobacillus acidipiscis*, *Akkermansia muciniphila*, and *Rothia* spp. were significantly higher at the development stage (W1 to W7), while decreased from W9 and reached an extremely low level at W56 and W111 (Fig. 3c). Some genus was only higher in adulthood (W7–W12) including *Turicibacter* spp. and *Lactobacillus reuteri*.
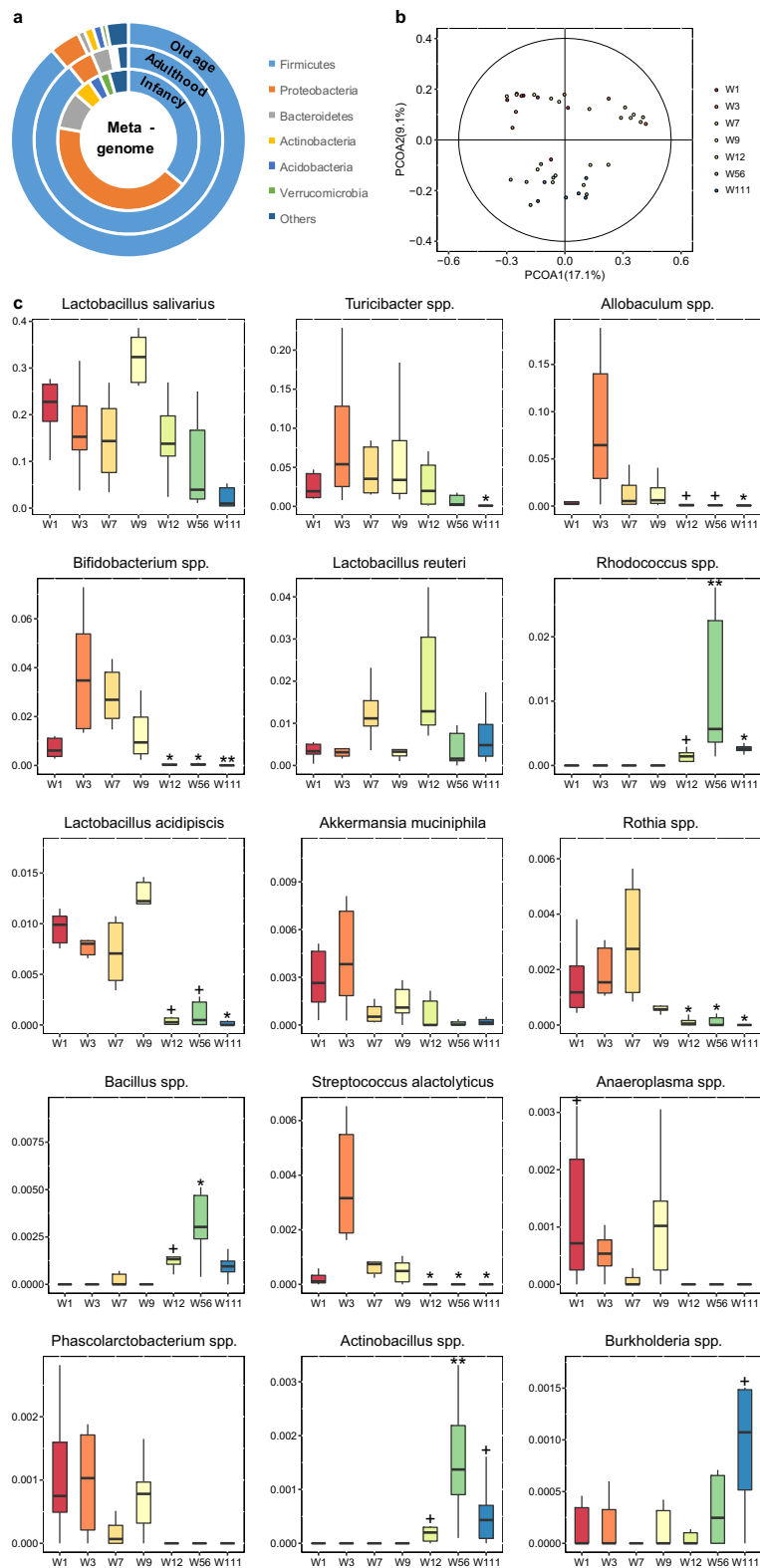
◀ **Fig. 3** The effects of age on the microbial composition. **a** The relative abundance of bacterial phyla in infancy, adulthood, and old age. The pie charts were normalized by sample groups. **b** The principal coordinate analysis (PCoA) performed based on the mean-centered values of unweighted UniFrac matrix. **c** The boxplots of the relative abundance of significantly changed genera and species in rats among the lifespan ($n = 6$). $^+p < 0.05$, $*p < 0.01$, and $**p < 0.001$ when compared with W7 by Dunn's test

Correlation analysis of metabolome and microbiome

In the high-level association study, we performed two different strategies for dimensionality reduction. For the knowledge-driven dimensionality reduction, the heatmap in Fig. 4a shows the correlation between metabolite types and gut microbiome functional pathways (details of each category in Table S2). The black-bordered square marks indicate the parts that are significantly related to age, and their change trend with age is shown in Fig. 4b.

For the data-driven dimensionality reduction, using the newly reported computational platform (Pedersen et al. 2018), we collapsed metabolites and gut microbiota data into 12 and 10 clusters, respectively, and the every individual metabolite and bacterium that within each cluster was summarized in Table S3 and Table S4. The metabolic and bacterial clusters that most related to age were M01 ($r = -0.870$, $p = 9.98 \times 10^{-13}$) and B05 ($r = -0.774$, $p = 1.84 \times 10^{-08}$), respectively. The M01 includes three amino acids proline, 4-hydroxyproline, and lysine, which were all decreased with age (Table S3). The B05 includes several probiotics, such as *Rothia* spp., *Bifidobacterium* spp., *Lactobacillus acidipiscis*, and *Enterococcus* spp., which were significantly negatively correlated with age (Table S4). Then the clusters were taken forward for cross-domain association analyses (Fig. 5). Also, the M01 was positively correlated with B05 ($r = 0.651$, $p = 4.28 \times 10^{-05}$).

In the low-level association study, the association between individual metabolite and gut microbiota was performed and is shown in Fig. S2. Several associations between metabolites and microbiota were identified at an FDR of 0.05. In this heatmap, a variety of age-related metabolites, including 4-hydroxyproline, tetradecanoate, dodecanoate, decanoate, and benzoate, were significantly correlated with gut genus. Tetradecanoate, dodecanoate, and decanoate were positively correlated with *Glycomyces* spp., *Olivibacter* spp., *Phascolarctobacterium* spp., *Pedobacter* spp., *Phenylobacterium* spp., etc. *in B04*; and *Sphingobium* spp., *Anaeroplasma* spp., *Chitinophaga* spp., and *Cellvibrio* spp. in B06.

### Correlation analysis on metabolites, bacterium, and immune factors

The alterations of immune factors and cytokines among the lifespan are illustrated in Fig. S3; they are represented by "factors" hereby. In addition, cytokines and immune indicator levels did not change a lot with age, except for IL-2 which showed a decreasing trend with age (Fig. S3). At the last time point, a few factors showed significant differences within group, indicating differences in the immune status of the elderly (Fig. S3).

The percentage of two related variable pairs (bacteria-metabolites, immune factor-bacteria, and immune factor-metabolites) is shown in Fig. 6a, showing that the correlations between immune factors and metabolome declined with age. Details of age-specific correlations are listed in Fig. S4, indicating amino acids, fatty acids, and TCA participants showed high correlations with immune factors in childhood period.

The associated relationship between immune factors and metabolites, as well as gut microbiota in whole samples (whole ages), was conducted and is displayed in Fig. S2. The complex network in Fig. 6b summarized complicated relationships among the changes of key variables, showing that IL-10, IgM, IgA, 4-hydroxyproline, and tetradecanoate were crucial nodes, including local correlation groups such as tetradecanoate-decanoate-dodecanoate, IgG-cysteine, and 4-hydroxyproline-IgA. In general, amino acids and long-chain fatty acids showed a stronger association with immune factors and cytokines. Succinate, malate, fructose, benzoate, and long-chain fatty acids including tetradecanoate, dodecanoate, and decanoate were positively correlated with IgM, but most of them were negatively correlated with IL-10 (Fig. S2). IgA is proportional to inosine and inversely proportional to 4-hydroxyproline and proline (Figs. 6b and S2).

In the correlation analysis between gut bacteria and factors, we only found that IL-10, IgM, IgA, IgG, and NK were significantly correlated to gut bacteria (Figs. 6 and S2). Specifically, IL-10 was positively related to a variety of bacteria, such as *Lactobacillus* spp., *Lactobacillus reuteri*, *Bacillus* spp., and *Flavobacterium succinicans*, and negatively related to most of gut genera, especially *Cellvibrio* spp., *Clostridium* spp., and *Clostridium celatum*. IgA in the spleen was positively

Fig. 4 Correlation analysis results of the knowledge-driven metabolite type-bacterial function across the lifespan. **a** The Spearman correlation coefficient for metabolite types and metabolic functions of microbiome ($^+p < 0.05$, $*p < 0.01$). **b** The scatter plots with correlation coefficients of selected metabolite types and metabolic functions ($n = 6$)
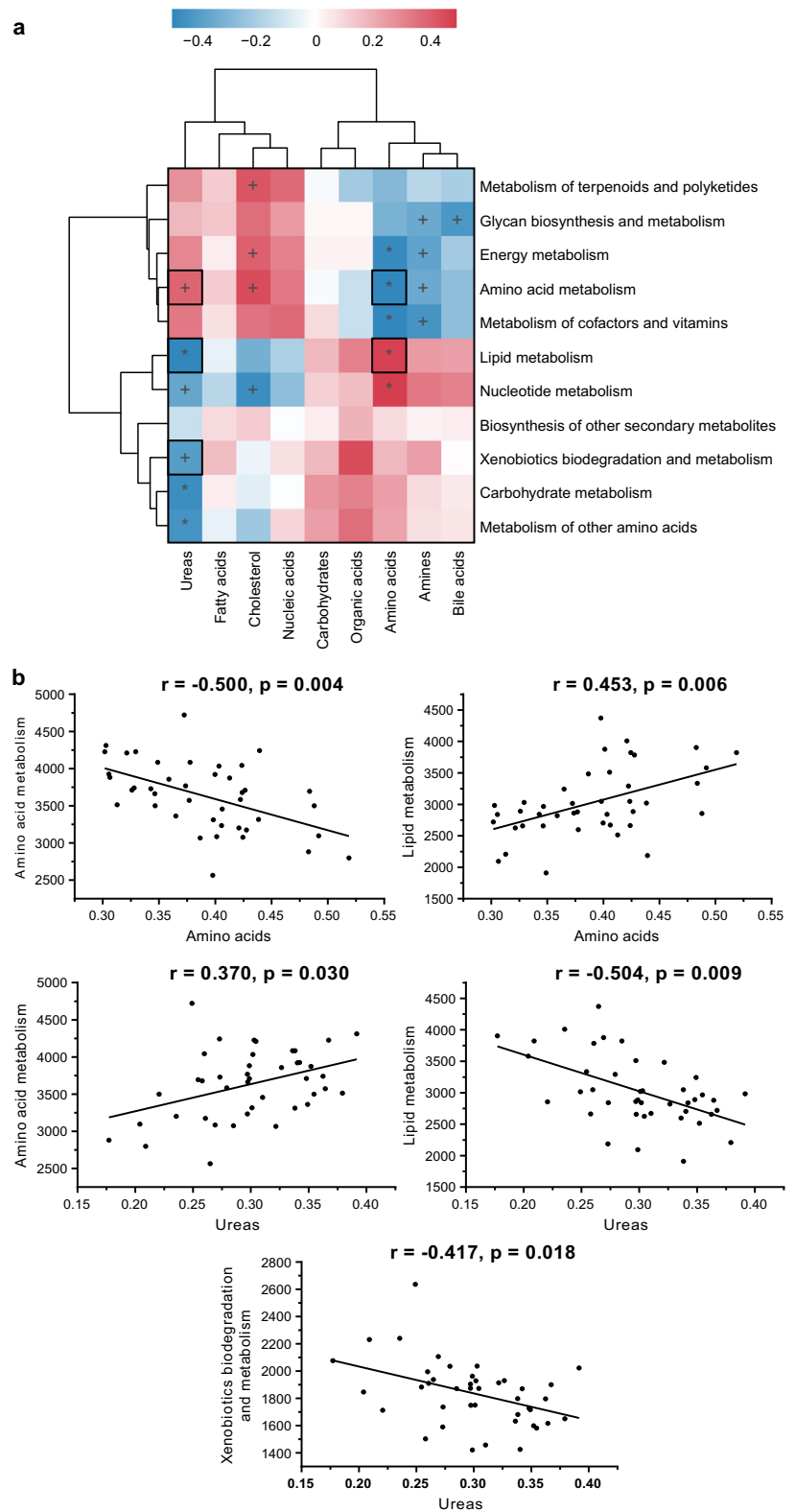
correlated with *Flavobacterium succinicans*, *Actinobacillus* spp., *Cupriavidus* spp., *Rhizobium* spp., *Rhodococcus* spp., and *Salinispora* spp. and negatively correlated with *Rothia* spp., *Bifidobacterium* spp., *Enterococcus* spp., and *Candidatus Arthromitus*, indicating that immune factors are highly related to ileal flora.

Discussion

The gut microbiota is associated with the immune system factors which are important contributing factors to age-related degenerative diseases (Biragyn and Ferrucci 2018). Compared with mice, experimental rat gut metagenome showed a higher pairwise overlap with humans than that between mice and humans at the gene level (Pan et al. 2018). In our previous studies, we demonstrated metabolic deviation in different brain regions due to aging (Zheng et al. 2016) and investigated the correlation between intestinal flora and brain metabolites in rats (Chen et al. 2018). Brain metabolism showed significant shifts in different life stages of rats. Similar results were also reported in the current study. Serum metabolite levels varied differently at early ages (W1–W9) compared with those at an older age (W12, W56, and W111) (Fig. 2). These changes at 9 weeks were associated with the rat's maturation. In infancy, minimal carbohydrate (saccharides and glycols) levels are detected, and then, they reach normal levels in adulthood and remain unchanged or slightly increased in old age (Fig. 2d). However, fatty acids were shown to be at higher levels in the early stages of life (Fig. 2e). Glycerol and fatty acids are significantly higher in the early stages of life compared with older stages, and this has been associated with the breast milk diet (Dessì et al. 2018). Among the three most abundant phyla in the ileum, Firmicutes have been shown to gradually increased with age, while the others showed different trends (Fig. 3a). It can be inferred that the difference in diet is one of the reasons for the differences in gut flora at infancy. In addition, disorders associated with flora disturbance result in the regulation of energy metabolism and the accumulation of excessive fat in old age (Maier et al. 2017).

Serum amino acid level displayed a positive correlation with nucleic acid and lipid metabolism; amino acids had a negative correlation with amino acid and vitamin metabolism (Fig. 4), indicating that gut bacteria might have complementary effect on amino acid production

(Dodd et al. 2017).There is a similar relationship between ureas and multiple pathways of gut bacteria, as it was proven that the supplement with prebiotics and probiotics significantly increased uric acid and decreased urea and urea nitrogen levels in blood (Firouzi and Haghighatdoost 2018). This correlation results in Fig. 4 illustrated an overall interaction of circulating metabolites and gut flora's metabolism function.

Our results showed 4-hydroxyproline having the most significant changes among the metabolites due to the significant decline after aging (Fig. 2c), and also an important node in the correlation network (Fig. 6b). One of the significant characteristics of old age is the loss of collagen, while 4-hydroxyproline is a decomposition product of collagen. Furthermore, the results showed that serum 4-hydroxyproline levels gradually decreased with age. Age-related probiotics in the B05 bacterial group (Fig. 5, details in Fig. S2 and Table S4) including *Rothia* spp., *Bifidobacterium* spp., *Lactobacillus acidipiscis*, and *Enterococcus* spp. were shown to be positively correlated with 4-hydroxyproline. It has been reported that 4-hydroxyproline metabolic enzymes exist widely in the gut microbiota, which participate its metabolism with the host (Huang et al. 2018). So it could be inferred that the collagen metabolism is partly impacted by aging caused by changes in the microbiota. In the cluster M01 (Fig. 5, details in Fig. S2 and Table S3), proline and lysine showed similar trends with 4-hydroxyproline (Fig. 2c). These two amino acids are also closely related to aging and inflammation (Nepal et al. 2018). While in cluster M11, gluconate and glucuronate decreased in old age. In addition, infants' serum levels of myo-inositol and citrate were found to be significantly lower than those in adults (Fig. 2d). This indicates that energy metabolism is slowed down by aging.

Cysteine, a precursor of the anti-oxidant glutathione with multiple physiological functions, was found to be significantly declined in both infancy and old age (Fig. 2c). Oxidative stress induces abnormal cysteine oxidation in aging and neurodegenerative diseases and also affects protein function (Gu and Robinson 2016). This confirms the need for cysteine supplementation for infants, old adults, and even people with certain metabolic diseases (McCarty and DiNicolantonio 2015). In this study, cysteine was positively correlated with *Bifidobacterium* spp., *Desulfovibrio* spp., and *Streptococcus alactolyticus* (Fig. 6, details in Fig. S2). Studies have shown that the expressions of cysteine biosynthetic

a
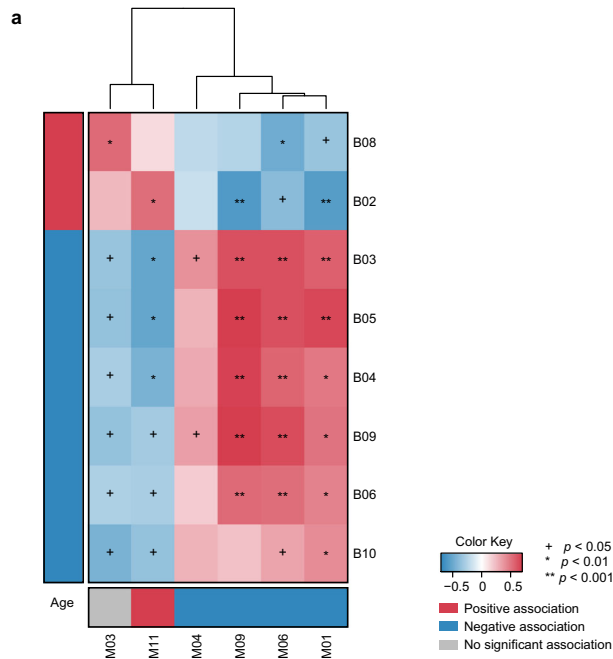
Partial clustering categories of metabolites and gut bacteria

M01	4-Hydroxyproline, Proline, Lysine
M02	Serine, Tryptophan, Valine, Leucine, Ornithine, Phenylalanine
M04	Isoleucine, Malate, Succinate
M05	Cysteine
M06	Methionine, Tetradecanoate
M07	Ferulate
M08	Docosahexaenoate
M09	Fructose, Benzoate, Dodecanoate, Decanoate
M10	Inosine
B03	*Akkermansia* muciniphila, *Actinomyces* spp., *Streptococcus* spp., *Acinetobacter* johnsonii
B04	*Glycomyces* spp., *Olivibacter* spp., *Phascolarctobacterium* spp., *Pedobacter* spp., *Phenylobacterium* spp., etc,
B05	*Rothia* spp., *Bifidobacterium* spp., *Lactobacillus* acidipiscis, *Enterococcus* spp.
B06	*Sphingobium* spp., *Anaeroplasma* spp., *Chitinophaga* spp., *Cellvibrio* spp.

Note: The whole categories were shown in Table S3 and Table S4

b
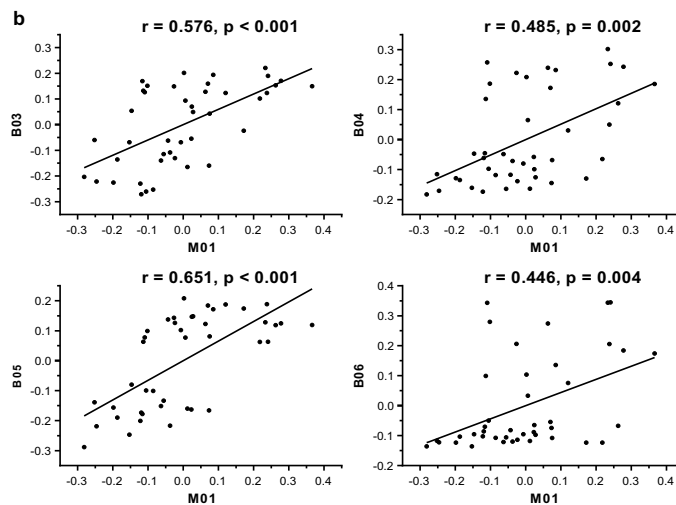
Fig. 5 Correlation analysis results of the data-driven metabolic clusters-bacterial clusters across the lifespan. **a** The Spearman correlation coefficient for metabolic clusters-bacterial clusters. **b** The scatter plots with correlation coefficients of metabolites and gut microbiota clusters derived from the computational platform. The left and bottom panels show associations between clusters and age. Colors indicates the association direction with age (red: positive; blue: negative; gray: not significant). The right panel shows associations between the metabolomic clusters and bacterial clusters. The clusters with not at least one significant association were excluded. In this study, 6 metabolic clusters and 8 bacterial clusters were kept

genes are very important for *Bifidobacteria* growth (Ferrario et al. 2015). A recent study suggested an antagonistic relationship between sulfur-reducing bacteria and *Bifidobacterium* spp., which compete for cysteine (Malmuthuge et al. 2019). In this study, *Bifidobacterium* sp. content and cysteine were low during the first week of life. With the increase in abundance of *Bifidobacterium* spp., cysteine was also increased, and then, they were found to both decrease in old age. Therefore, it could be inferred that supplementation of *Bifidobacterium* spp. or cysteine may promote each other and help improve metabolic disorders in old age.

The levels of an aromatic amino acid (including phenylalanine, tyrosine, and tryptophan) and branched-chain amino acid (BCAA, including isoleucine, leucine, and valine) were shown to be increased from W9 to W111 (Fig. 2c), whereas higher levels of circulating BCAA were associated with insulin resistance and the development of diabetes and have been reported as predictors of cardiovascular diseases (Chen et al. 2016; Magnusson et al. 2013; Wang et al. 2011). Correlation analysis results revealed that branched-chain amino acids and their metabolites, ornithine and phenylalanine, were found to be positively correlated with IL-10 (Figs. 6b and S2). It was reported that branched-chain amino acid affects immune functions and even the concentration of IL-10 (De Simone et al. 2013). IL-10 is believed to regulate aging-related inflammation by affecting insulin resistance, while maintaining high levels of IL-10 may help to enhance body vitality and resist aging (Dagdeviren et al. 2017; Jankord and JEMIOLO 2004). In this correlation network diagram (Fig. 6b), IL-10 is located at a crucial node of the network, which is associated with multiple metabolites and enteric bacteria. Recent studies have reported that inflammatory factors are regulated by a variety of metabolites, such as methionine and serine (Yu et al. 2019). Methionine was found to be positively correlated with IgG, while

ferulate was positively whereas serine was negatively correlated with IgG and NK (Figs. 6 and S2).

Notably, the W1 group had higher abundance of all fatty acids detected in the serum than other age groups (Fig. 2e), indicating that fatty acids participate in the development of rats at infant stage. The decline in fatty acids from W1 to W7 revealed rapid consumption from infant to adulthood. In our results, the abundance of docosahexaenoate (DHA), elaidiate, and linoleate gradually increased from W9 to W111. Previous study reported that elaidiate is elevated in obese individuals and those with metabolic syndrome (Gil-Campos et al. 2008; Kim et al. 2013). Circulating PUFAs affect host inflammation state (Perreault et al. 2014; Steffen et al. 2012). It has been proven that DHA have an effect on IL-2 signaling pathways (Gorjão et al. 2013). Our results show a positive association between docosahexaenoate (DHA) and inflammatory IL-2, and both of them were isolated from the whole network (Fig. 6b), while other long-chain fatty acids such as tetradecanoate, dodecanoate, and decanoate were positively correlated with *Phascolarctobacterium* spp. in B04, *Anaeroplasma* spp. and *Cellvibrio* spp. in B06, and *Akkermansia* muciniphila in B03. *Akkermansia muciniphila* was reported to regulate metabolism balance and immune tolerance (Greer et al. 2016; Plovier et al. 2017). Recent studies have shown that *Phascolarctobacterium* spp. produce propionate and are associated with dietary intervention among vulnerable elderly people (O'Hara et al. 2018; Tran et al. 2019). Anaeroplasma was also associated with polyunsaturated fatty acid feeding and positively correlates with acetic acid level in rat brains (Nguyen et al. 2019; Robertson et al. 2017). Furthermore, tetradecanoate, dodecanoate, and decanoate were all associated with IgM and "tetradecanoate-decanoate-dodecanoate-IL-10-IgM" formed a local close connection in Fig. 6b, reflecting the possible interaction between immune factors and metabolites.

The line chart of correlated pairs in Fig. 6a revealed that the percentage of significantly correlated factor-metabolite pairs is higher in the early stages of life declined with age (infancy). In particular, amino acids, fatty acids, and TCA participants such as citrate and malate showed higher correlations (Fig. S4). This is probably due to the fact that infants require an external diet intake to support the establishment of a mature immune system (Rijkers et al. 2010). It should be noted that all the pair (factor-bacteria, factor-metabolites,
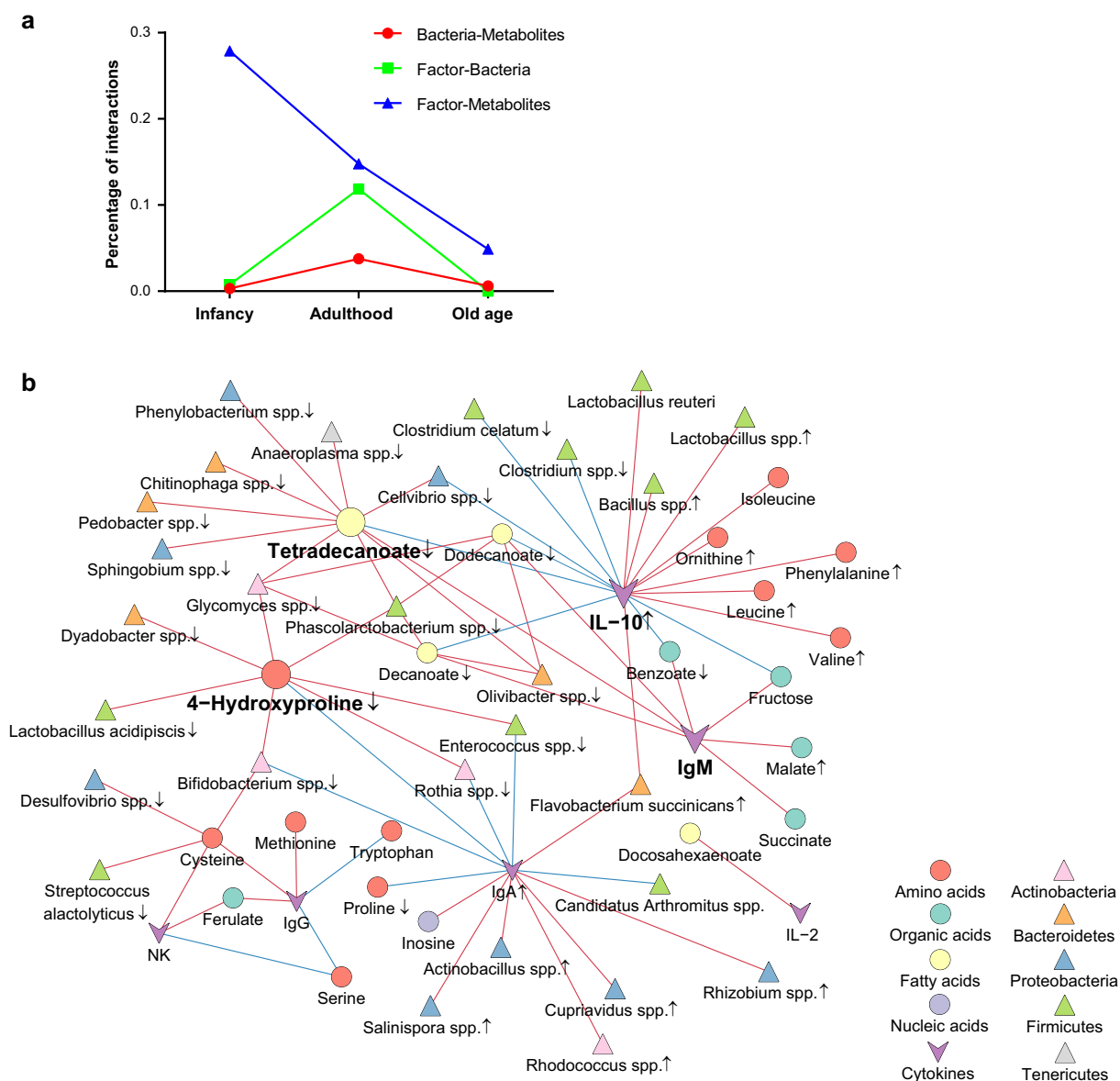
Fig. 6 Correlation analysis results of the low-level dual-omics data. **a** The percentage line chart of significantly correlated pairs with age. Infancy: W1 + W3; adulthood: W7 + W9 + W12; old age: W56 + W111. **b** The interactions between meta significant correlated pairs of metabolite-microbiota-factors. Lines in red and blue represent positive and negative correlations, respectively; upwards arrow: positively related to age; downwards arrow: negatively related to age

bacteria-metabolites) correlations are decreased in old age (Fig. S4), which may be the result of too large variation within the group due to the inconsistent aging process of individuals.

Previous studies have shown that intestinal flora regulates some peripheral circulating cytokines, which also influence the structure of gut flora (Biancheri and Watson 2017). The result showed that spleen IL-10 was positively related to a variety of bacteria, such as *Lactobacillus* spp. and *Lactobacillus* reuteri (Figs. 6b and S2), since IL-10 has been implicated in the maintenance of gut homeostasis (Ray et al. 2015). Probably it does this by regulating probiotics including *Lactobacillus*. As for IgA, studies have shown that secretory IgA affects mucosal bacterial communities (Donaldson et al. 2018). Recent research also demonstrates that plasma IgA

reacts brings about different gut flora structures (Grosserichter-Wagener et al. 2019). Our result showed that IgA in the spleen was positively correlated with *Actinobacillus* spp. and *Rhodococcus* spp. and negatively correlated with *Rothia* spp., *Bifidobacterium* spp., and *Enterococcus* spp., indicating that immune factors are highly related to ileal flora as well. Although IgM could help IgA to promote highly diverse commensal communities of gut mucosa, spleen IgM was not directly related to a certain group of bacteria in this study (Magri et al. 2017).

In summary, this comprehensive dual-omics aging study identified key metabolites, gut bacteria, immune factors, and cytokines varying across the lifespan. Our findings provide new insights into the interactions between circulating metabolites and gut bacteria functional metabolism pathways. A two-level strategy associate study establishes network links of key metabolites (as 4-hydroxyproline, cysteine); several beneficial gut bacteria including *Bifidobacterium*, *Lactobacillus*, and *Akkermansia*; and IgA, IgM, and IL-10 during the growth, development, and aging of rats.

Compliance with ethical standards All experiments were carried out strictly in accordance with recommendations on the National Institutes of Health's Guide for Care and Use of Laboratory Animals. The experimental program was approved by the Center for Laboratory Animals of Shanghai Jiao Tong University.

References

Bárcena C, Valdés-Mas R, Mayoral P, Garabaya C, Durand S, Rodríguez F, et al. Healthspan and lifespan extension by fecal microbiota transplantation into progeroid mice. Nat Med. 2019;25:1234–42.

Biancheri P, Watson AJM. The relative contributions of the gut microbiome, host genetics, and environment to cytokine responses to microbial stimulation. Gastroenterology. 2017;152:2068–70.

Biragyn A, Ferrucci L. Gut dysbiosis: a potential link between increased cancer risk in ageing and inflammaging. Lancet Oncol. 2018;19:e295–304.

Bolyen E et al. (2018) QIIME 2: reproducible, interactive, scalable, and extensible microbiome data science. PeerJ Preprints,

Buford TW. (Dis) Trust your gut: the gut microbiome in age-related inflammation, health, and disease. Microbiome. 2017;5:80.

Butler RN, Miller RA, Perry D, Carnes BA, Williams TF, Cassel C, et al. New model of health promotion and disease prevention for the 21st century. Bmj. 2008;337:a399.

Callahan BJ, McMurdie PJ, Rosen MJ, Han AW, Johnson AJA, Holmes SP. DADA2: high-resolution sample inference from Illumina amplicon data. Nat Methods. 2016;13:581–3.

Castaneda-Delgado JE, et al. Differences in cytokine production during aging and its relationship with antimicrobial peptides production. Immunol Investig. 2017;46:48–58.

Chen T, Ni Y, Ma X, Bao Y, Liu J, Huang F, et al. Branched-chain and aromatic amino acid profiles and diabetes risk in Chinese populations. Sci Rep. 2016;6:20594.

Chen T, You Y, Xie G, Zheng X, Zhao A, Liu J, et al. Strategy for an association study of the intestinal microbiome and brain metabolome across the lifespan of rats. Anal Chem. 2018;90: 2475–83.

Chen Y, Li Z, Tye KD, Luo H, Tang X, Liao Y, et al. Probiotics supplementation during human pregnancy affects the gut microbiome and immune status. Front Cell Infect Microbiol. 2019;9:254.

Dagdeviren S, Young Jung D, Friedline RH, Noh HL, Kim JH, Patel PR, et al. IL-10 prevents aging-associated inflammation and insulin resistance in skeletal muscle. FASEB J. 2017;31: 701–10.

De Simone R, Vissicchio F, Mingarelli C, De Nuccio C, Visentin S, Ajmone-Cat MA, et al. Branched-chain amino acids influence the immune properties of microglial cells and their responsiveness to pro-inflammatory signals. Biochim Biophys Acta. 2013;1832:650–9.

DeSantis TZ, et al. Greengenes, a chimera-checked 16S rRNA gene database and workbench compatible with ARB. Appl Environ Microbiol. 2006;72:5069–72.

Dessì A, Briana D, Corbu S, Gavrili S, Cesare Marincola F, Georgantzi S, et al. Metabolomics of breast milk: the importance of phenotypes. Metabolites. 2018;8:79.

Dodd D, Spitzer MH, van Treuren W, Merrill BD, Hryckowian AJ, Higginbottom SK, et al. A gut bacterial pathway metabolizes aromatic amino acids into nine circulating metabolites. Nature. 2017;551:648–52.

Donaldson G et al. (2018) Gut microbiota utilize immunoglobulin A for mucosal colonization. Science (80-) 360:795–800.

Douglas GM et al. (2019) PICRUSt2: an improved and extensible approach for metagenome inference. BioRxiv:672295.

Ferrario C, et al. Exploring amino acid auxotrophy in Bifidobacterium bifidum PRL2010. Front Microbiol. 2015;6:1331.

Ferrucci L, Fabbri E. Inflammageing: chronic inflammation in ageing, cardiovascular disease, and frailty. Nat Rev Cardiol. 2018;15:505–22.

Firouzi S, Haghighatdoost F. The effects of prebiotic, probiotic, and synbiotic supplementation on blood parameters of renal function: a systematic review and meta-analysis of clinical trials. Nutrition. 2018;51:104–13.

Gil-Campos M, del Carmen R-TM, Larque E, Linde J, Aguilera CM, Canete R, et al. Metabolic syndrome affects fatty acid

composition of plasma lipids in obese prepubertal children. Lipids. 2008;43:723–32.

Gorjão R, Hirabara S, Cury-Boaventura M, de Lima T, Passos M, Levada-Pires A, et al. Signaling pathways involved in the effects of different fatty acids on interleukin-2 induced human lymphocyte proliferation. J Clin Cell Immunol. 2013;4: 171.

Greer RL, Dong X, Moraes ACF, Zielke RA, Fernandes GR, Peremyslova E, et al. Akkermansia muciniphila mediates negative effects of IFNγ on glucose metabolism. Nat Commun. 2016;7:13329.

Grosserichter-Wagener C, Radjabzadeh D, van der Weide H, Smit KN, Kraaij R, Hays JP, et al. Differences in systemic IgA reactivity and circulating Th subsets in healthy volunteers with specific microbiota enterotypes. Front Immunol. 2019;10:341.

Gu L, Robinson RA. Proteomic approaches to quantify cysteine reversible modifications in aging and neurodegenerative diseases. Proteomics Clin Appl. 2016;10:1159–77.

Hor YY, et al. Lactobacillus sp. improved microbiota and metabolite profiles of aging rats. Pharmacol Res. 2019;146:104312.

Hou Y, Wang X, Lei Z, Ping J, Liu, Ma Z, et al. Heat-stress-induced metabolic changes and altered male reproductive function. J Proteome Res. 2015;14:1495–503.

Huang YY, Martinez-Del Campo A, Balskus EP. Anaerobic 4-hydroxyproline utilization: discovery of a new glycyl radical enzyme in the human gut microbiome uncovers a widespread microbial metabolic activity. Gut Microbes. 2018;9:437–51.

Jankord R, JEMIOLO B. Influence of physical activity on serum IL-6 and IL-10 levels in healthy older men. Med Sci Sports Exerc. 2004;36:960–4.

Kim OY, Lim HH, Lee MJ, Kim JY, Lee JH. Association of fatty acid composition in serum phospholipids with metabolic syndrome and arterial stiffness. Nutr Metab Cardiovasc Dis. 2013;23:366–74.

Korpela K, Dikareva E, Hanski E, Kolho K-L, De Vos WM, Salonen A. Cohort profile: Finnish Health and Early Life Microbiota (HELMi) longitudinal birth cohort. BMJ Open. 2019;9:e028500.

Kurilshikov A, van den Munckhof ICL, Chen L, Bonder MJ, Schraa K, Rutten JHW, et al. Gut microbial associations to plasma metabolites linked to cardiovascular phenotypes and risk. Circ Res. 2019;124:1808–20.

Langfelder P, Horvath S. WGCNA: an R package for weighted correlation network analysis. BMC Bioinformatics. 2008;9: 559.

Magnusson M, Lewis GD, Ericson U, Orho-Melander M, Hedblad B, Engström G, et al. A diabetes-predictive amino acid score and future cardiovascular disease. Eur Heart J. 2013;34: 1982–9.

Magri G, et al. Human secretory IgM emerges from plasma cells clonally related to gut memory B cells and targets highly diverse commensals. Immunity. 2017;47:118–134. e118.

Maier TV, Lucio M, Lee LH, VerBerkmoes NC, Brislawn CJ, Bernhardt J, et al. Impact of dietary resistant starch on the human gut microbiome, metaproteome, and metabolome. MBio. 2017;8.

Malmuthuge N, Liang G, Griebel PJ, Guan LL. Taxonomic and functional compositions of the small intestinal microbiome in neonatal calves provide a framework for understanding early life gut health. Appl Environ Microbiol. 2019;85.

McCarty MF, DiNicolantonio JJ. An increased need for dietary cysteine in support of glutathione synthesis may underlie the increased risk for mortality associated with low protein intake in the elderly. Age (Dordr). 2015;37:96.

Nepal M, Ma C, Xie G, Jia W, Fei P. Fanconi Anemia complementation group C protein in metabolic disorders. Aging (Albany NY). 2018;10:1506–22.

Nguyen TD, Prykhodko O, Fak Hallenius F, Nyman M. Monovalerin and trivalerin increase brain acetic acid, decrease liver succinic acid, and alter gut microbiota in rats fed high-fat diets. Eur J Nutr. 2019;58:1545–60.

O'Hara E, Kelly A, McCabe MS, Kenny DA, Guan LL, Waters SM. Effect of a butyrate-fortified milk replacer on gastrointestinal microbiota and products of fermentation in artificially reared dairy calves at weaning. Sci Rep. 2018;8:14901.

Pan H, Guo R, Zhu J, Wang Q, Ju Y, Xie Y, et al. A gene catalogue of the Sprague-Dawley rat gut metagenome. Gigascience. 2018;7.

Pedersen HK, Forslund SK, Gudmundsdottir V, Petersen AØ, Hildebrand F, Hyötyläinen T, et al. A computational framework to integrate high-throughput '-omics' datasets for the identification of potential mechanistic links. Nat Protoc. 2018;13:2781–800.

Perreault M, Zulyniak MA, Badoud F, Stephenson S, Badawi A, Buchholz A, et al. A distinct fatty acid profile underlies the reduced inflammatory state of metabolically healthy obese individuals. PLoS One. 2014;9:e88539.

Plovier H, Everard A, Druart C, Depommier C, van Hul M, Geurts L, et al. A purified membrane protein from Akkermansia muciniphila or the pasteurized bacterium improves metabolism in obese and diabetic mice. Nat Med. 2017;23:107–13.

Ray A, Basu S, Gharaibeh RZ, Cook LC, Kumar R, Lefkowitz EJ, et al. Gut microbial dysbiosis due to helicobacter drives an increase in marginal zone B cells in the absence of IL-10 signaling in macrophages. J Immunol. 2015;195:3071–85.

Rijkers GT, Niers L, Stasse-Wolthuis M, Rombouts FM (2010) Nutrition, the infant and the immune system. In: Dietary Components and Immune Function. Springer, pp 3–23.

Robertson RC, Seira Oriach C, Murphy K, Moloney GM, Cryan JF, Dinan TG, et al. Deficiency of essential dietary n-3 PUFA disrupts the caecal microbiome and metabolome in mice. Br J Nutr. 2017;118:959–70.

Sansoni P, Vescovini R, Fagnoni F, Biasini C, Zanni F, Zanlari L, et al. The immune system in extreme longevity. Exp Gerontol. 2008;43:61–5.

Singh H, Torralba MG, Moncera KJ, DiLello L, Petrini J, Nelson KE, Pieper R (2019) Gastro-intestinal and oral microbiome signatures associated with healthy aging. Geroscience.

Steffen BT, Steffen LM, Tracy R, Siscovick D, Hanson NQ, Nettleton J, et al. Obesity modifies the association between plasma phospholipid polyunsaturated fatty acids and markers of inflammation: the Multi-Ethnic Study of Atherosclerosis. Int J Obes. 2012;36:797–804.

Ticinesi A, Nouvenne A, Tana C, Prati B, Meschi T. Gut microbiota and microbiota-related metabolites as possible biomarkers of cognitive aging. Adv Exp Med Biol. 2019;1178: 129–54.

Tran TT, et al. Prebiotic supplementation in frail older people affects specific gut microbiota taxa but not global diversity. Microbiome. 2019;7:39.

Wang TJ, Larson MG, Vasan RS, Cheng S, Rhee EP, McCabe E, et al. Metabolite profiles and the risk of developing diabetes. Nat Med. 2011;17:448–53.

Wijsman CA, Rozing MP, Streefland TCM, le Cessie S, Mooijaart SP, Slagboom PE, et al. Familial longevity is marked by enhanced insulin sensitivity. Aging Cell. 2011;10:114–21.

Yu W, et al. One-carbon metabolism supports S-adenosylmethionine and histone methylation to drive inflammatory macrophages. Mol Cell. 2019;75:1147–1160.e1145.

Zhang Z, Wang X, Wang J, Jia Z, Liu Y, Xie X, et al. Metabonomics approach to assessing the metabolism variation and endoexogenous metabolic interaction of ginsenosides in cold stress rats. J Proteome Res. 2016;15: 1842–52.

Zheng X, Chen T, Zhao A, Wang X, Xie G, Huang F, et al. The brain metabolome of male rats across the lifespan. Sci Rep. 2016;6:24125.